In Situ STM Study of Cu(111) Surface Structure and Corrosion in Pure and Benzotriazole-Containing Sulfuric Acid Solution

W. Polewska,† M. R. Vogt, O. M. Magnussen,* and R. J. Behm

Abteilung Oberflächenchemie und Katalyse, Universität Ulm, D-89069 Ulm, Germany

Received: June 10, 1999; In Final Form: September 22, 1999

We present results of an in situ STM study on the surface structure and anodic dissolution of Cu(111) electrodes in pure 0.01 M H_2SO_4 solution and in solution containing the corrosion inhibitor benzotriazole (BTAH), which is aimed at an atomistic understanding of the dissolution process and the inhibitior effects. The initial stages of Cu dissolution as well as the adsorption of BTAH are pronouncedly influenced by the presence of the ordered sulfate adlayer, which forms in the double layer potential regime and induces a reconstruction of the underlying Cu surface layer, together with a reorientation of the steps along the close-packed lattice directions. Cu dissolution in pure H_2SO_4 solution proceeds by a step flow mechanism. The onset of dissolution is critically affected by the relative orientation of the sulfate adlayer on the lower terrace side, with the stability being highest for steps running perpendicular to the close-packed sulfate rows. The retracting steps often expose apparently disordered areas, which are attributed to a disordered sulfate adlayer on a Cu surface where, because of kinetic limitations, a well-ordered reconstruction has not yet reformed. BTAH adsorption is only observed in the potential regime of the ordered sulfate adlayer. The BTAH adlayer is highly defective, which is attributed to the removal of the reconstruction due to sulfate adlayer displacement. Islands with poorly ordered 1D chain structures are surrounded by areas with no resolved structure. Cu dissolution inhibition is manifested by an anodic shift in the onset of dissolution as well as by the blocking of the step flow etch mechanism, reflecting a stabilization of the Cu steps by adsorbed BTAH. Dissolution at higher potentials proceeds predominantly via formation of monolayer etch pits. When the potential is reversed back into the double layer regime, smoothening of the surface is observed with a rate that increases strongly with decreasing potential.

1. Introduction

Anodic Cu dissolution in aqueous solutions has been investigated in numerous studies because of its practical importance in Cu corrosion and electrorefinement as well as because of fundamental interest in electrochemical metal dissolution/deposition reactions.[1] Most of these studies concentrated on the macroscopic kinetics of this process and its dependence on electrolyte composition and the effect of corrosion-inhibiting organic additives, such as benzotriazole (BTAH, $C_6H_4N_3H$). For a better understanding of the underlying atomic scale processes, model studies have been performed on the dissolution of Cu single-crystal electrodes in pure acidic solutions using electrochemical and ex situ techniques[2−4] and, more recently, in situ scanning probe techniques, such as atomic force microscopy (AFM)[5,6] and scanning tunneling microscopy (STM).[7−12] Likewise, to understand the microscopic mechanism underlying the inhibiting properties of the technologically important corrosion inhibitor BTAH, the chemisorption of BTAH on copper and cuprous oxide surfaces has been investigated extensively in model studies in the electrochemical environment as well as under ultrahigh vacuum (UHV) conditions.[13−21] These studies show that at low coverages or negative potentials BTAH forms a chemisorbed adlayer on top of the Cu surface, whereas at higher coverages or more positive potentials, a multilayer phase consisting of a polymerized Cu(I)−BTA complex is formed that protects the Cu surface against corrosion.[13−16]

Previous studies revealed pronounced differences in the dissolution and inhibition behavior for different anions such as sulfate or chloride. Less clear, however, is the influence of crystallographic effects, i.e., the influence of the Cu surface structure on these processes. The atomic scale mechanisms of Cu dissolution have been studied on two different surfaces, Cu(111)[7] and Cu(100),[8−12] in pure HCl solution. In sulfuric acid, in contrast, similar model studies on Cu dissolution were only performed on Cu(100),[10] whereas on Cu(111) such studies were restricted to the double layer potential regime.[22−26] Also, the influence of the substrate orientation on the microscopic mechanism of corrosion inhibition by organic additives has not been investigated yet. So far, only a single study exists, where the effect of the crystallographic orientation on the inhibition efficiency was investigated and where an increasing BTAH inhibition efficiency in the order (111), (110), and (100) was suggested.[2]

We recently reported results of a detailed in situ scanning tunneling microscopy (STM) study on the surface structure and anodic dissolution of Cu(100) electrodes in pure and BTAH-containing sulfuric and hydrochloric acid solutions.[9,10,27−29] These experiments revealed in detail how the structure of the anion adlayer, in particular that of the ordered $c(2 \times 2)$ Cl^- adlayer, influences the dissolution mechanism and gave a wealth of data on the BTAH adlayer formation, on the structure of the BTAH adlayer at (sub-) monolayer and multilayer coverages, and on the Cu dissolution/deposition processes in the presence of BTAH.[27−29] With increasing BTAH coverage individual

† Permanent address: Institute of Physics, Poznan University of Technology, Ul. Piotrowo 3, 60-965 Poznan, Poland.

10.1021/jp991903l CCC: $18.00
Published on Web 11/05/1999

chainlike BTAH aggregates, islands of two ordered adlayer phases, a $(^2/_3\ ^1/_3)$ superstructure with unit cell vectors of $(5)^{1/2}d_{Cu}$ and $(13)^{1/2}d_{Cu}$ ($d_{Cu} = 2.55$ Å) and a (5×5)R26.6° superstructure, and a multilayer phase consisting of randomly arranged molecular chains were observed. From the nearest-neighbor spacing within these structures, an adsorption geometry could be inferred where the BHAH molecules are arranged in parallel stacks with the molecular plane being perpendicular or slightly tilted with respect to the surface normal. In sulfuric acid solution it was found that the BTAH adlayer is present on the Cu(100) surface in the entire double layer potential range up to the onset of Cu corrosion and that even submonolayer BTAH islands significantly inhibit the removal of Cu atoms along the steps.[27,29] In contrast, in HCl solution the BTAH adlayer is present on the surface only at negative potentials whereas at more positive potentials it is displaced by the ordered $c(2 \times 2)$ Cl^- adlayer, which explains the well-known reduction of the BTAH inhibition efficiency in the presence of this anion.

Here, we present a high-resolution in situ STM study of Cu(111) electrodes in pure and BTAH-containing sulfuric acid solution, which gives detailed data on the surface structure and morphology in the double layer range and on the mechanisms of Cu dissolution and redeposition. In contrast to Cu(100), where the sulfate is apparently adsorbed in the form of a disordered layer of highly mobile adsorbates in the entire double layer potential range,[27] on Cu(111) the potential-induced formation of a complex superstructure attributed to an ordered sulfate adlayer was recently reported by various groups.[23−26] In this study we will give first results on the influence of this adlayer on the mechanism of Cu(111) dissolution and on the formation of the BTAH adlayer. In particular, we will show how the presence of this anion adlayer pronouncedly affects the (defect) structure of the BTAH adlayer and consequently the Cu dissolution mechanism in BTAH-containing H_2SO_4 solution. These microscopic observations are correlated with corresponding electrochemical measurements.

2. Experimental Section

The measurements were performed using a home-built STM, described in detail in ref 30, and electrochemically etched W tips coated with Apiezon wax. Sample and tip potentials were controlled potentiostatically with respect to a Hg/Hg_2SO_4 (K_2SO_4 sat.) reference electrode. All potentials in this paper, however, are quoted versus the saturated calomel electrode (SCE) for easier comparison with our previous results. STM images were taken at constant current mode with tunneling currents from 0.6 to 4 nA and are displayed as gray scale images with lighter colors corresponding to higher surface locations.

The procedures for sample preparation were identical to those used previously in the experiments on Cu(100).[27] At the beginning of each experiment the Cu(111) single crystal, which was already mounted in the STM cell, was electropolished in 66% orthophosphoric acid at potentials around 2.4 V vs the Pt counter electrode. Subsequently, it was rinsed with ultrapure water, covered with pure 0.01 M sulfuric acid (Merck, suprapure), and mounted in the STM at an initial potential in the range −0.50 to −0.20 V. After assessing the quality and cleanness of the surface in the pure sulfuric acid solution, varying amounts of solution containing 10^{-4} M BTAH (Fluka, puriss.) were added, resulting in BTAH-concentrations of 1×10^{-6} to 2×10^{-4} M. Because of the small cell volume and large electrode surface area, a concentration of 10^{-5} M corresponds to a coverage of 1 ML (with respect to the number of Cu surface atoms) after complete adsorption of all BTAH in the solution.

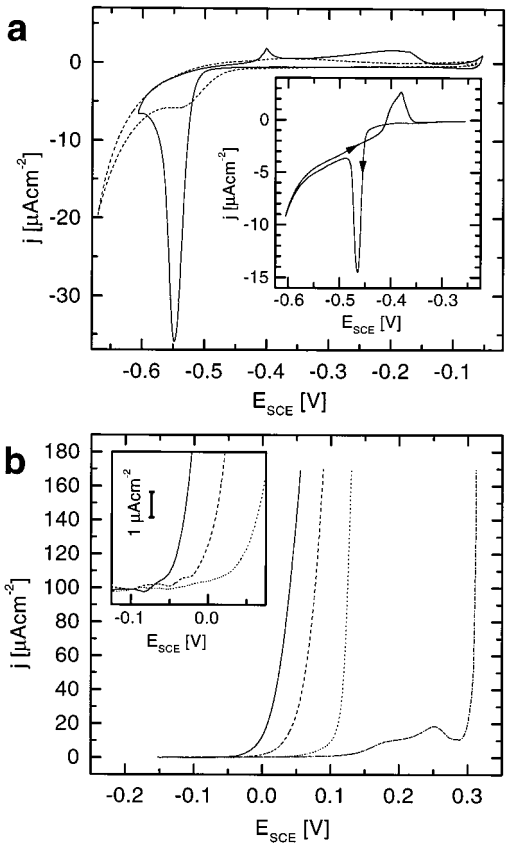

Figure 1. Current−potential curves of Cu(111) in 0.01 M H_2SO_4 containing no (solid line), 10^{-6} M (dashed line), 10^{-4} M (dotted line), and 10^{-2} M (dashed−dotted line) BTAH showing (a) the double layer potential regime (potential sweep rate, 5 mV/s; sweep rate in inset, 1 mV/s) and (b) Cu dissolution (potential sweep rate, 0.5 mV/s).

3. Results

3.1. Electrochemical Measurements. Prior to the STM experiments electrochemical current−voltage curves of Cu(111) in pure and BTAH-containing 0.01 M H_2SO_4 solution were recorded, which are shown in Figure 1. The curves were obtained in a separate electrochemical cell in deaerated electrolyte using the dipping technique. The Cu(111) electrode was prepared in the same way as in the STM experiments.

Cyclic voltammograms, recorded in the double layer regime between −0.60 and −0.05 V in pure 0.01 M H_2SO_4 solution, show a pronounced cathodic peak with the peak maximum between −0.46 and −0.55 V (depending on the scan rate) and corresponding very broad anodic features at potentials above −0.42 V (Figure 1a). The voltammograms were completely reproducible without any changes even after extended cycling. These observations agree completely with previous results, where those features were assigned to the desorption and adsorption of an ordered sulfate adlayer[23,24] (for details see below). On the basis of detailed measurements at various scan rates between 1 and 20 mV s^{-1}, we conclude that the features in the anodic scan result from a fast process, reflected by a scan-rate-independent peak at −0.40 V, and a second process with very slow kinetics, which can be attributed to surface reorganization (see below). As shown in the inset in Figure 1a, both peaks merge at very slow scan rates. Even then, however, they are shifted by ∼80 mV relative to the cathodic peak. In addition, the inset in Figure 1a reveals in the potential range from −0.45 to −0.42 V three to five times lower current densities in the cathodic scan, where the surface is covered by the ordered adlayer, as compared to the anodic scan, where the sulfate

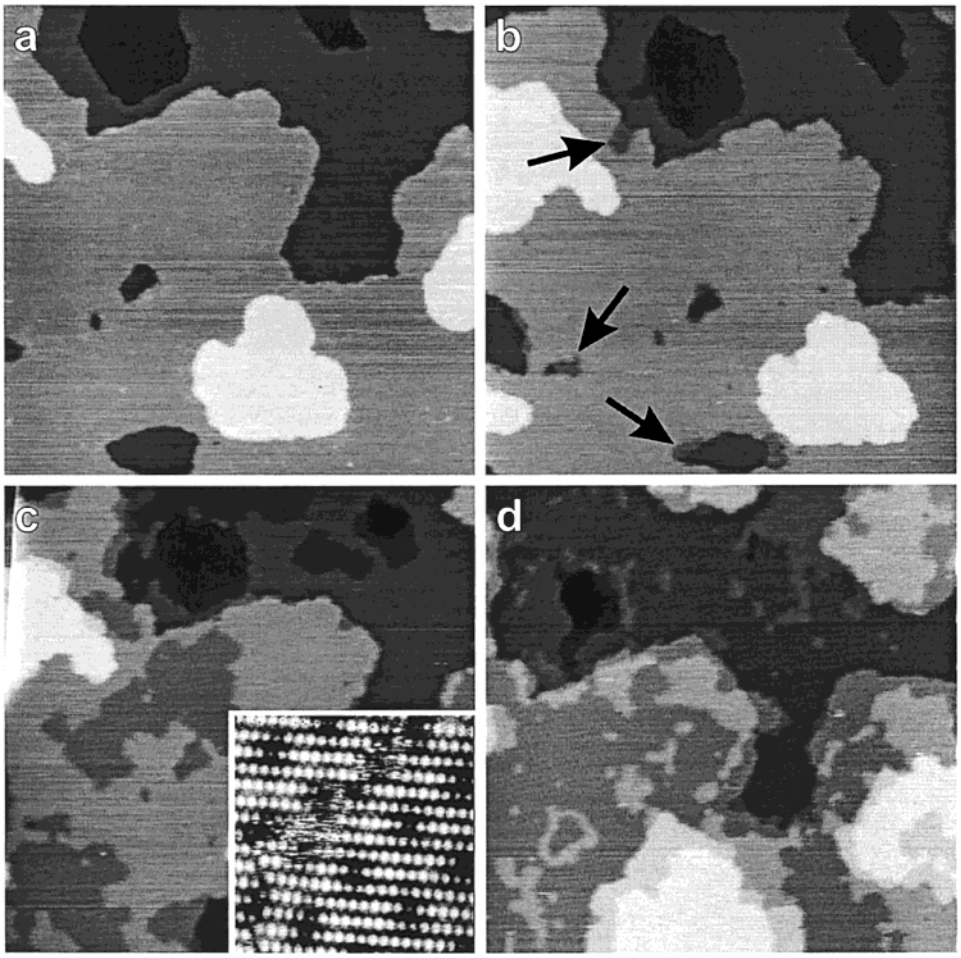

Figure 2. Series of STM images (1650 × 1650 Å^2, I_t = 2 nA) showing the formation of sulfate adlayer on Cu(111) in 0.01 M H_2SO_4: (a) clean Cu(111) surface at −0.51 V, (b−d) the nucleation and growth of the ordered sulfate adlayer (b) at −0.41 V, (c) 5 min later at −0.40 V, and (d) additional 3 min later at −0.39 V. The inset in (c) (100 × 100 Å^2) shows the molecular lattice of the adsorbate as well as the Moire pattern.

adlayer is disordered. Hence, the hydrogen evolution reaction is strongly suppressed in the presence of the ordered sulfate adlayer. This observation is at variance with the interpretation given by Wilms et al.,[24] according to whom the ordered sulfate adlayer enhances hydrogen evolution.

The presence of BTAH causes clear changes in the voltammograms. They become visible already at very low BTAH concentrations, as evidenced by the voltammograms recorded in 0.01 M H_2SO_4 solution containing 10^{-6} M BTAH (Figure 1a, dashed line). Although the characteristic features are still visible, in particular the cathodic peak at −0.55 V, the charge associated with the anodic and cathodic peaks is much weaker, indicating that only a small part of the surface is covered by the sulfate adlayer. The latter conclusion is supported also by the increased current at potentials below −0.60 V, which suggests that the hydrogen evolution reaction is less blocked under these conditions. These observations can be explained by the presence of an incomplete BTAH adlayer. At higher BTAH concentrations the peaks corresponding to the adsorption/desorption of the sulfate adlayer are completely suppressed and only a constant double layer charging current without adsorption/desorption peaks is found.

The Cu(111) dissolution behavior was studied in more detail by current−voltage curves at lower potential scan rates ("polarization curves"), i.e., under quasi-static conditions (Figure 1b). In inhibitor-free solution these experiments show an exponentially increasing Cu dissolution current at potentials positive of −0.05 V (Figure 1b, solid line). The onset of Cu dissolution in the current−voltage curve is, within 10 mV, identical to that measured under identical conditions on Cu(100) electrodes.[29] In electrolytes containing small amounts of BTAH the onset of Cu(111) dissolution is shifted to significantly more positive potentials. For example, shifts of about 80 and 150 mV are observed at BTAH concentrations of 10^{-6} and 10^{-4} M, respectively (see enlarged scale in Figure 1b, inset, dashed and dotted line). Again, this behavior is almost identical to that observed on Cu(100). For solutions containing ≥0.01 M BTAH the shifts in the onset of Cu dissolution become even larger (∼0.3 V for 10^{-2} M). Furthermore, a broad peak between 0.15 and 0.28 V is observed. Again, this behavior resembles observations for Cu(100) in H_2SO_4 and HCl solutions at high BTAH concentrations and can be attributed to the formation of a thick passivating Cu(I)BTA layer. These data seem to suggest that the crystallographic orientation has no significant effect on the kinetics of the Cu dissolution process in pure and BTAH-containing sulfuric acid solution.

3.2. STM Studies of Cu(111) in Pure Sulfuric Acid. In situ STM observations of the Cu(111) surface in pure sulfuric acid within the double layer potential range are in complete agreement with the results of a previous detailed study by Wilms et al.[23,24] As seen in the series of STM images in Figure 2, smooth terraces separated by monatomically high Cu steps are visible at potentials between −0.60 and −0.50 V (Figure 2a). After the sample potential was increased to about −0.40 V, the formation of islands of the ordered sulfate adlayer is observed (Figure 2b,c). Atomic resolution images of this adlayer (see inset

in Figure 2c) show the characteristic structure, i.e., a distorted hexagonal lattice with nearest- and next-nearest-neighbor distances of 4.5 ± 0.5 and 7 ± 0.5 Å, respectively, superimposed by a long-range vertical modulation (Moiré pattern). The areas covered by the ordered phase can be easily recognized in the STM images because of the long-range Moiré pattern and their 0.9 Å lower apparent height (i.e., darker appearance) in comparison to the surrounding Cu surface. As is shown in Figure 2b (see arrows), these areas nucleate predominantly at step edges from where they slowly grow over the terraces (Figure 2c) until the entire surface is covered by this structure (Figure 2d). The rate of this process is low at -0.40 V but increases strongly with increasing potential. Presumably, the slow process found in the anodic scan of the voltammogram corresponds to this ordered adlayer growth (the scan-rate-independent peak at -0.40 V might be caused by sulfate adsorption on the (1×1) Cu(111) surface). The formation of the sulfate adlayer is accompanied by Cu mass transport, resulting in growth of the Cu terraces along the steps and in the appearance of copper islands on top of previously smooth terraces (see parts b and c of Figure 2). Conversely, the formation of monatomic pits in the terraces and an opposite rearrangement of the steps is found during the dissolution of the ordered adlayer after decreasing the potential to values less than -0.45 V. These phenomena were observed and described previously and attributed to a sulfate-induced reconstructive expansion of the topmost Cu layer, which leads to the release of Cu atoms onto the surface.[23,24] In addition, the formation of the ordered adlayer induces a faceting of the Cu steps with the steps oriented along the close-packed directions of the Moiré structure, similar to the effect of the ordered Cl adlayers on Cu(100)[8,9,11,29] and Cu(111).[7]

The dissolution behavior of Cu(111) in pure sulfuric acid solution is illustrated by the STM images in Figure 3, which were selected from a continuous series recorded in the same surface area. Figure 3a shows the initial Cu surface at a potential in the double layer range with several terraces separated by monatomically high Cu steps. In addition, a screw dislocation can be found near the lower edge of the image (marked by a circle in Figure 3a−f), which has a fixed position and hence can be used as a landmark during the dissolution process. The terraces are completely covered by extended domains of the sulfate superstructure with the Moiré pattern and the rowlike molecular fine structure clearly visible (the smaller distance of 4.5 Å is not resolved because of the large image size). Subsequently, the potential was stepwise increased to -0.13 V (Figure 3b). At this potential Cu dissolution begins via removal of atoms along some of the Cu steps, e.g., at the position marked by a black arrow in Figure 3b. The step faceting along the close-packed directions of the Moiré structure, which is dominant in the double layer regime, disappears in the later stages of the corrosion process. When the potential is maintained at this value (Figure 3c,d), continuous local dissolution as well as local growth of Cu terraces (see, for example, the arrow in Figure 3c) due to Cu redeposition occur. Interestingly, these dissolution/redeposition processes do not proceed with equal probability at all steps but are only observed at some of them while others are almost unchanged (examples of the latter are marked by white arrows in Figure 3b). The different stability of steps against Cu dissolution can be linked to local differences in the adlayer structure, in particular, to the orientation of the ordered sulfate adlayer on the adjacent lower terraces. It turns out that the steps with the close-packed rows of the sulfate adlayer ("$\sqrt{3}$" direction) being approximately perpendicular to the step direction (Figure 3b, white arrows) are more stable than the steps running approximately parallel to those rows (Figure 3b, black arrow).

Parallel to the onset of Cu dissolution, the adlayer structure changes visibly. Areas that do not exhibit the ordered adlayer structure but are covered by a second, apparently disordered phase emerge on the surface (see, for example, upper right corner of Figure 3d). The STM images show no difference in the apparent height of this new phase relative to that of the ordered sulfate adlayer. Areas of the new, disordered phase are found preferentially on the lower terrace side of Cu steps and, to a much smaller extent, at domain boundaries of the ordered sulfate adlayer. With longer etching times, an increasing fraction of the terraces is covered by these areas. The Moiré pattern cannot be discerned in the disordered phase; however, small patches of only a few 10 Å in diameter, which show the molecular structure of the ordered sulfate adlayer, are found to briefly emerge and disappear again in these disordered areas (see, for example, arrow in Figure 3d). A detailed inspection of the images reveals that domains of the disordered phase form preferentially on the lower terrace side of those steps where pronounced dissolution/redeposition processes are observed, whereas for the more stable steps the adjacent lower terrace exhibits the ordered adlayer structure (see white arrows in Figure 3b). In contrast, the adlayer structure on the adjacent upper terrace, i.e., on the dissolving terrace, does not seem to affect the dissolution behavior. Possible explanations for these observations will be given in section 4.

At even more positive potentials (Figure 3e,f), around -0.10 V, the growth of the disordered areas and consequently the fraction of the surface covered by this phase as well as the rate of the dissolution/redeposition processes at the steps increase. The potential regime and local dissolution rates of this process are very similar to those observed for the dissolution/redeposition of Cu(100) in 0.01 M H_2SO_4 solution. In comparison to the latter, however, the steps on the Cu(111) surface remain smoother and the fluctuations in the step positions are less pronounced during the dissolution process than on Cu(100). In clean sulfuric acid solution and in the studied potential regime (below -0.05 V) Cu(111) dissolution proceeds solely by this step flow mechanism. The formation of etch pits in the middle of the Cu terraces was not observed under these conditions.

When the potential is stepped back to more negative values, the disordered areas gradually disappear and domains of the ordered sulfate adlayer reappear, which, however, may exhibit a shape and orientation different from those present on the surface prior to the potential excursion to positive values. This indicates that the order in the sulfate adlayer is really destroyed in the disordered phase rather than being obscured by an additional dissordered adlayer on top. The time required for the complete re-formation of the ordered structure depends on the potential and is on the order of a few seconds for potentials below -0.30 V.

On Cu(111) electrodes that exhibit a higher density of surface defects such as Cu adislands or domain boundaries in the ordered adlayer (e.g., as in Figure 2d), the overall mechanism of the step flow etch process is rather similar. Cu islands are dissolved at the very onset of Cu dissolution (at potentials above -0.17 V), which results in the transient formation of disordered areas but does not seem to affect the dissolution process. Furthermore, because of the higher defect density, the areas of the ordered and the disordered adlayer are typically much smaller and hence more difficult to distinguish in the STM

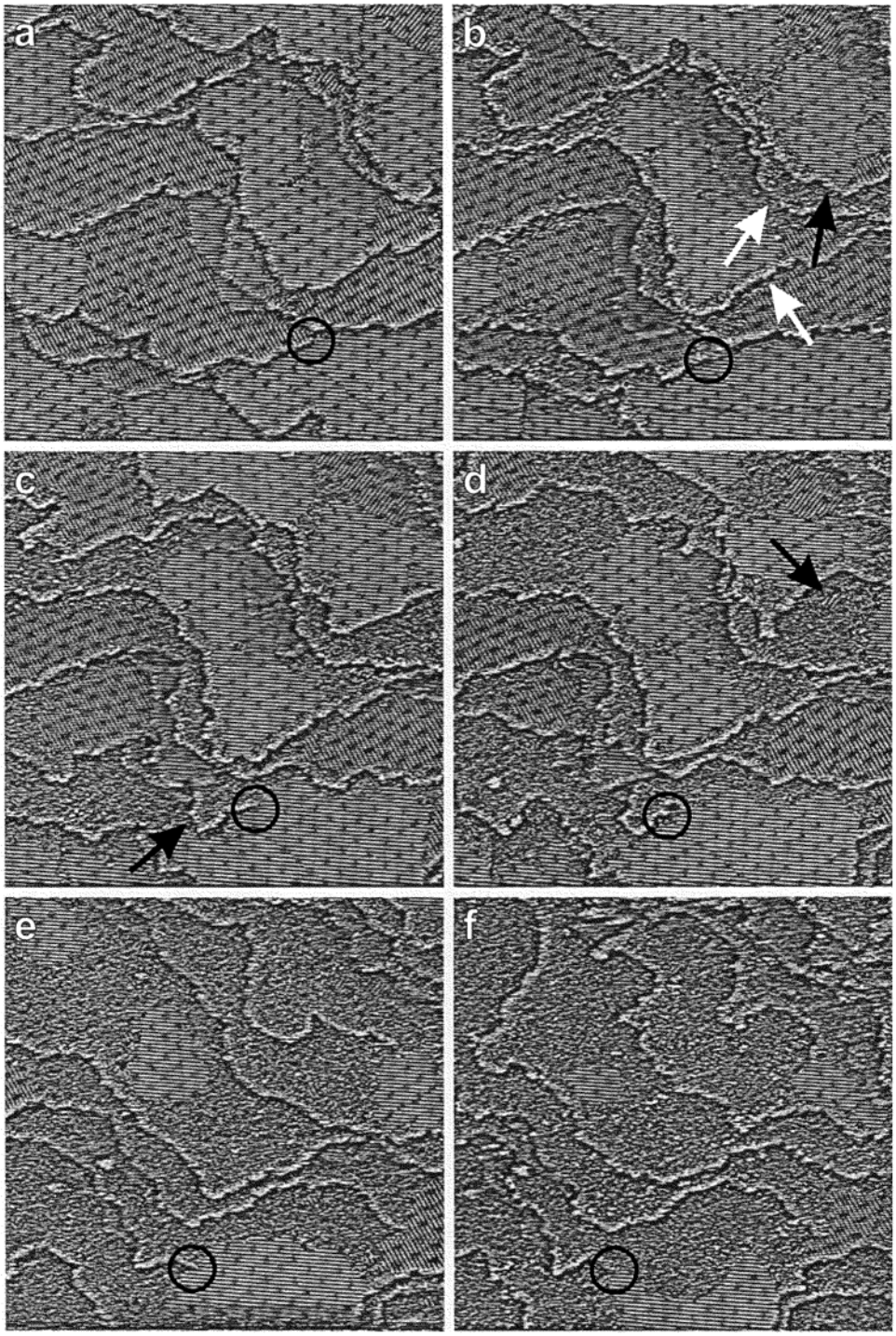

Figure 3. Series of STM images (700 × 780 Å^2, $I_t = 4$ nA) showing the dissolution of Cu(111) in 0.01 M H_2SO_4. For better visibility of the sulfate adlayer structure each terrace is colored by a separate gray scale; arrows are described in the text. The images are recorded (a) at −0.30 V (0 min), (b) at −0.13 V (7 min), (c) at −0.13 V (10 min), (d) at −0.13 V (12.5 min), (e) at −0.10 V (19.5 min), and (f) at −0.05 V (23.5 min).

images, resulting in a gradually more blurred appearance of the Moiré pattern.

3.3. STM Studies of Cu(111) in BTAH-Containing Sulfuric Acid Solution. After addition of BTAH to the solution, characteristic structural changes are observed on the Cu(111) surface in the double layer regime. At very low BTAH concentrations, where the BTAH coverage is ≤0.2 ML even after complete adsorption of all BTAH in the STM cell, structureless small islands with diameters of ≤50 Å are formed in the middle of the surrounding sulfate-covered surface (Figure 4a), which are attributed to BTAH adlayer islands. Their apparent height is between 0.6 and 1.3 Å relative to the surrounding ordered sulfate adlayer structure. Initially, these areas form predominantly at defects, such as Cu steps and domain boundaries of the sulfate superstructure (see upper right corner in Figure 4a). At higher BTAH concentrations in the electrolyte the sulfate adlayer structure is completely removed or suppressed and the surface is covered now by a phase, which appears uniform in larger scale images (see, for example, Figure 5a). High-resolution STM images such as Figure 4b, however, reveal pronounced local variations in the apparent height, with small (≤50 Å in diameter) BTAH islands being separated by

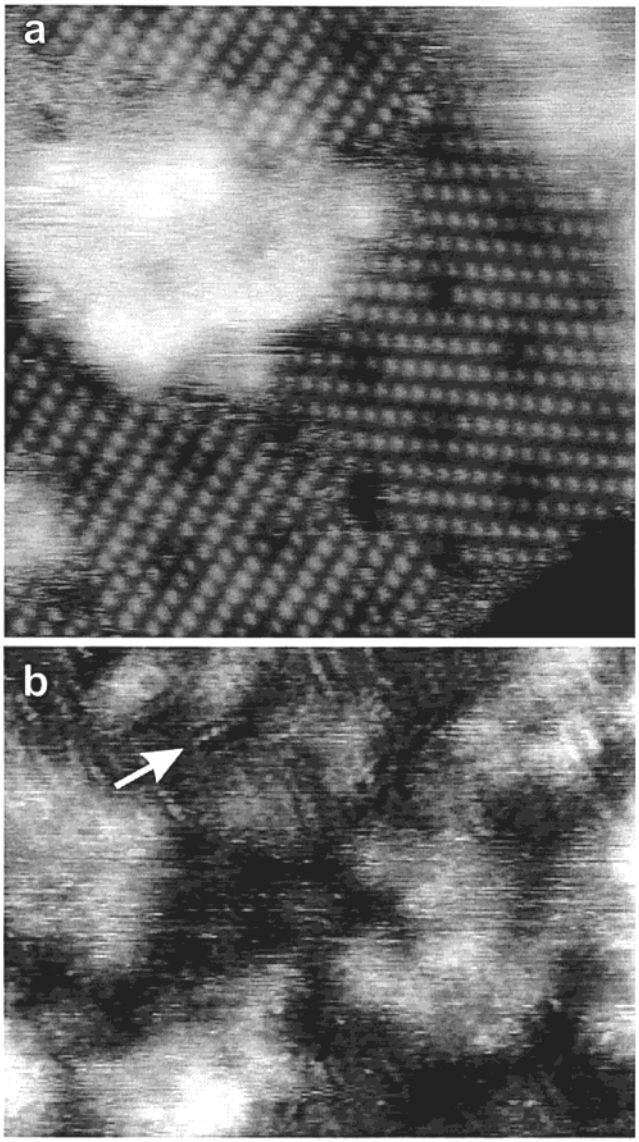

Figure 4. STM images showing the BTAH adlayer on Cu(111) (a) at submonolayer coverages (recorded in 0.01 M H_2SO_4 + 2 × 10^{-6} M BTAH at −0.45 V, 170 × 170 Å^2, I_t = 4 nA) and (b) for the full monolayer (recorded in 0.01 M H_2SO_4 + 10^{-5} M BTAH at −0.25 V, 250 × 110 Å^2, I_t = 0.6 nA).

0.5−1 Å lower depressions, rather than a homogeneous adlayer phase as on Cu(100). In some areas more or less parallel chains with a nearest-neighbor distance along the chains of ∼4 Å and a minimum spacing of ∼7 Å between neighboring chains can be resolved (see, for example, at the position marked by an arrow in Figure 4b). These findings resemble observations on BTAH-covered Cu(100) electrodes, where BTAH adlayer structures with similar intermolecular distances were found.[27−29] While the specific nature of the adsorbed BTAH species will be discussed later, it is clear that these structures indicate a BTAH-containing adlayer rather than a sulfate-covered surface.

The anodic dissolution of the Cu(111) electrode in BTAH-containing sulfuric acid solution is shown in the sequence of images in Figure 5, selected from a continuous series of data recorded in the same surface area. Starting from a potential in the double layer regime (Figure 5a), the potential was stepwise increased by about 25 mV every 2 min. The first changes in the surface morphology are observed at −0.08 V (Figure 5b). Cu dissolution commences by random removal of Cu atoms at steps, causing a step roughening, and by the formation of monatomically deep pits (marked by arrows). In Figure 5c, recorded 3 min later at −0.06 V, the pits have grown in size and second-layer etch pits have nucleated at the bottom of the larger pits, resulting in a gradual roughening of the surface. With time, this roughening continues (Figure 5d). Simultaneously, the images become increasingly "foggy" until no stable STM images can be obtained anymore. The latter behavior is similar to that found on Cu(100);[27,29] it is attributed to the formation of a Cu(I)BTA multilayer film with poor conducting properties.

The influence of the ordered sulfate adlayer on the formation of the BTAH adlayer as well as the inhibiting effect of chemisorbed BTAH on Cu(111) dissolution is illustrated by the sequence of STM images in Figure 6, recorded 30 min after adding BTAH (resulting in a concentration of 10^{-5} M) to the 0.01 M H_2SO_4 solution at a potential of −0.30 V. At the beginning of the experiment the potential was set to −0.54 V and then was very slowly increased in steps of 10 mV every 2 min. For potentials less than −0.40 V we observe the same surface morphology as in pure H_2SO_4 solution, with smooth terraces separated by monatomic steps (Figure 6a). No indications of a chemisorbed BTAH adlayer are found in this potential regime. Hence, the BTAH is either not yet adsorbed or it has a too high surface mobility to be detectable by STM. Structural changes are observed at −0.38 V (Figure 6b), where the ordered sulfate adlayer starts to form on the surface. The potential and the mechanism of this surface phase transition are identical to those in pure H_2SO_4 solution, suggesting again that BTAH is not yet adsorbed or only weakly interacting with the Cu substrate at this potential. Figure 6c shows the surface after complete formation of the ordered sulfate adlayer with the characteristic Moiré pattern and Cu monolayer islands created during this phase transition (see section 3.2). Other than in pure H_2SO_4 solution, however, there are also areas that appear ∼0.5 Å higher than the sulfate adlayer and that are attributed to BTAH-covered areas. These BTAH islands are found predominantly on the upper terrace side of most of the Cu steps. Interestingly, in some of the BTAH-covered areas the Moiré pattern seems to be still faintly recognizable (see inset in Figure 6c). Upon further increasing the potential at a rate of 25 mV per 3 min, no further morphological changes are observed up to −0.11 V. The formation of a complete BTAH adlayer was probably blocked in this experiment because of diffusional shielding by the STM tip, which (in contrast to the experiment shown in Figure 5) had been kept in the same surface location during the entire experiment (i.e., during the BTAH adsorption process). Cu dissolution commences at −0.09 V with the formation of small monatomic etch pits in the center of the terraces, in the areas (previously) covered by the ordered adlayer structure (Figure 6d). With increasing etch time, the size of these pits increases and additional pits nucleate both on the terraces and in existing pits (Figure 6e,f), similar to the experimental results in Figure 5. On the other hand there is no significant Cu dissolution at the steps, as can be seen for example at the position of the unusually shaped terrace shown in the inset in Figure 6c. This indicates that the steps are strongly stabilized by the BTAH adlayer.

Finally, we present an example of the potential-dependent smoothing of a Cu(111) electrode surface in the double layer range after this had been roughened by a potential excursion into the range of Cu dissolution (see sequence of STM images in Figure 7). This sequence is the continuation of the experiment shown in Figure 5, with Figure 7a being identical with Figure 5d. When the electrode potential is stepwise decreased (Figure 7b−f), the Cu surface becomes increasingly smooth until a

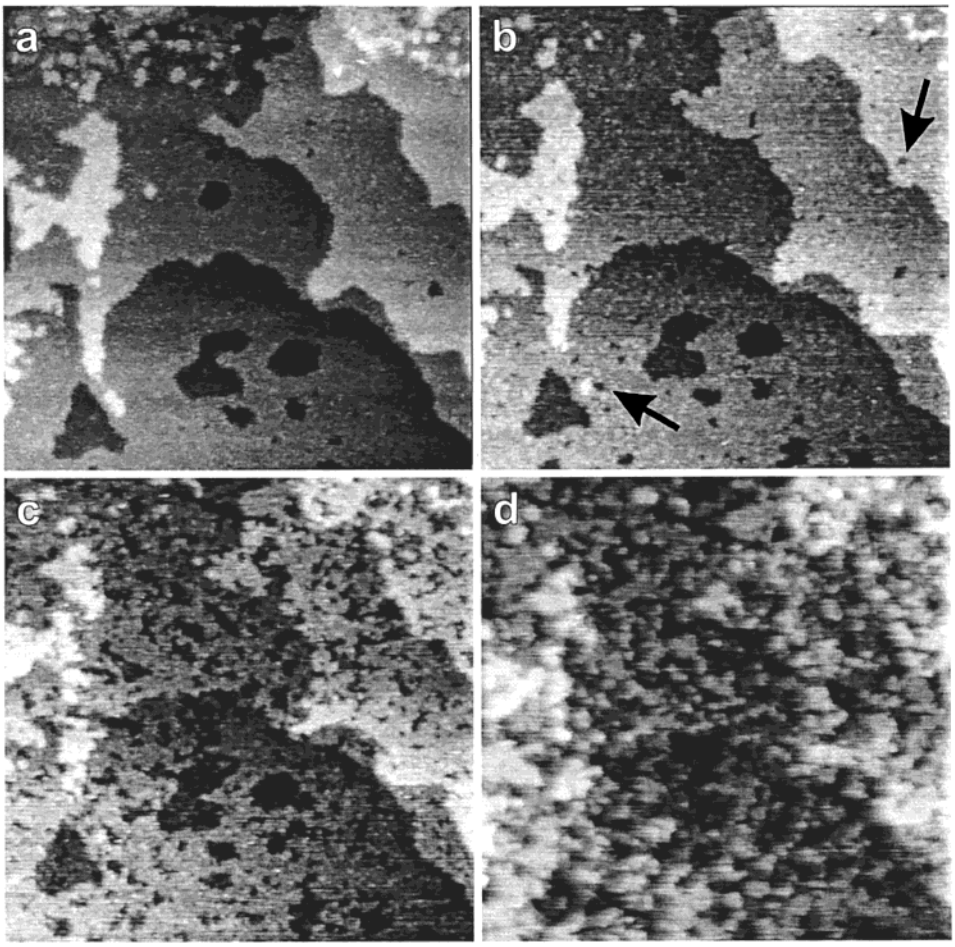

Figure 5. Series of STM images (1500 × 1500 Å^2, I_t = 1 nA) showing the anodic dissolution of Cu(111) in 0.01 M H_2SO_4 + 10^{-4} M of BTAH: (a) surface at −0.33 V before the onset of Cu dissolution; (b) start of etch pit formation after potential increase to −0.08 V; (c) 3 min and (d) 7 min later at −0.06 V.

perfectly flat Cu surface is regained. The smoothing process on the BTAH-covered surface proceeds via gradual filling of the etch pits, dissolution of Cu islands (see arrows in Figure 7e,f), and smoothing of the steps, all of which can be seen particularly well in the later stages of the smoothing (Figure 7e,f). This is distinctly different from the behavior in pure H_2SO_4 solution, where upon stepping the potential from the dissolution into the double layer range nucleation and growth of Cu monolayer islands due to redeposition are observed.[31] The rate of the BTAH-induced smoothing depends strongly on the potential and can be very fast at more negative potentials. For example, the transformation from a rough surface as in Figure 7a to a perfectly smooth surface as in Figure 7f requires only a few seconds if the potential is stepped from the dissolution regime to a value below −0.55 V. It should be noted that in this potential range, i.e., in the regime where the sulfate adlayer is disordered, a high surface mobility was also observed in BTAH-free H_2SO_4 solution, which impedes the assessment of the influence of BTAH. The Cu mass balance in the smoothing process seems to be relatively constant (within an error of ∼0.5 ML), in particular for fast potential steps, suggesting that this phenomenon is largely caused by Cu surface restructuring via surface diffusion. The growth of the terraces due to Cu redeposition from the solution is observed only on a slower time scale. A smoothing effect of BTAH on the Cu surface morphology was also found on Cu(100)[27] and may be the microscopic basis for the use of BTAH as an additive to Cu plating baths.

4. Discussion

The STM observations described above give new microscopic insight into the mechanisms of Cu(111) dissolution in pure and in BTAH-containing sulfuric acid solution. Similarities to (but also distinct differences from) Cu(100) in those electrolytes are found. In the following we will discuss in particular the influence of the ordered sulfate adlayer (a phenomenon not observed on the Cu(100) surface) on the processes of Cu(111) dissolution, BTAH adsorption, and BTAH-induced inhibition of Cu dissolution.

4.1. Cu(111) in Pure Sulfuric Acid Solution. The STM observations of the Cu(111) electrode structure in the double layer regime agree fully with the detailed, recent study by Wilms et al.[23,24] In particular, the same complex superstructure with an oblique unit cell and a long-range vertical modulation (Moiré pattern) is found. The same holds true for the mechanisms of the phase formation via nucleation and growth of the ordered structure, the emergence of Cu islands/pits accompanying the formation/dissolution of this phase, which is due to the reduced density of the underlying topmost Cu layer, and the electrochemical behavior, in particular the slow kinetics of ordered adlayer formation. According to the model proposed by those authors, the molecular arrangement of the sulfate adlayer is similar to that on other (111)-oriented metal surfaces.[32−34] The Moiré pattern is caused by a sulfate-induced reconstruction of the Cu surface layer, which is expanded by about 10%. As demonstrated by the electrochemical measurements in section 3.1, this ordered adlayer can significantly inhibit the hydrogen

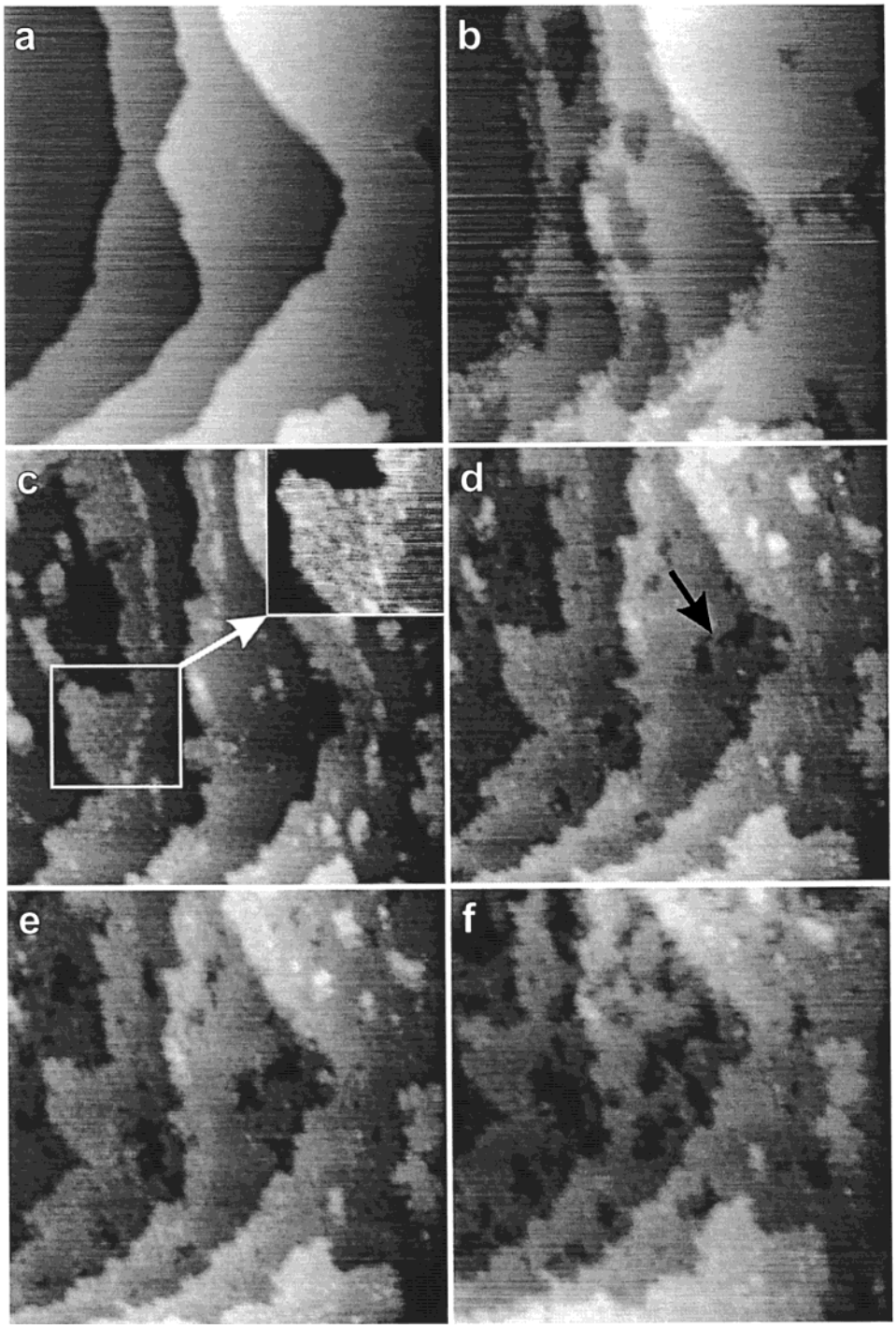

Figure 6. Series of STM images (1100 × 1100 Å^2, I_t = 0.8 nA) showing the interaction of BTAH with the ordered sulfate adlayer and Cu dissolution in the presence of BTAH submonolayer coverages on Cu(111) in 0.01 M H_2SO_4 + 10^{-5} BTAH: (a) initial Cu(111) surface at −0.44 V (0 min); ordered sulfate adlayer formation at (b) −0.38 V (6 min) and (c) −0.31 V (16 min); Cu dissolution in the surface areas not covered by BTAH at (d) −0.09 V (39 min), (e) −0.07 V (40 min), and (f) −0.06 V (42 min).

evolution reaction, indicating that it strongly affects the reactivity of the Cu(111) surface. To our understanding, the contrary results by Wilms et al.,[24] which were based on measurements at much higher potential sweep rates, are due to kinetic effects.

The dissolution of Cu(111) in pure H_2SO_4 solution likewise is much more complex than the dissolution of Cu(100) in this electrolyte,[10] which is again attributed to the presence of this sulfate adlayer and the related reconstruction of the Cu surface layer. Although on both surfaces a step flow etch mechanism is observed at sufficiently low dissolution rates, the dissolution/redeposition processes on the Cu(111) surface (i) do not occur uniformly along all steps as on Cu(100) but proceed at a different rate at different types of steps and (ii) are accompanied by the emergence of a new, apparently disordered adlayer phase. These differences will be discussed in the following, starting with the latter phenomenon. Most simply, the disordered phase can be explained by assuming that it involves a sulfate adlayer adsorbed on an unreconstructed (1 × 1) Cu substrate. Considering that the ordered sulfate layer is solely formed on a reconstructed Cu substrate with an expanded lattice,[23,24] or on other fcc(111) substrates with larger lattice constants such as Au(111),[32] Rh(111),[33] or Pt(111),[34] and that on the other side a disordered sulfate adlayer is formed on Cu(100), the smaller substrate lattice spacing of the unreconstructed Cu(111) surface

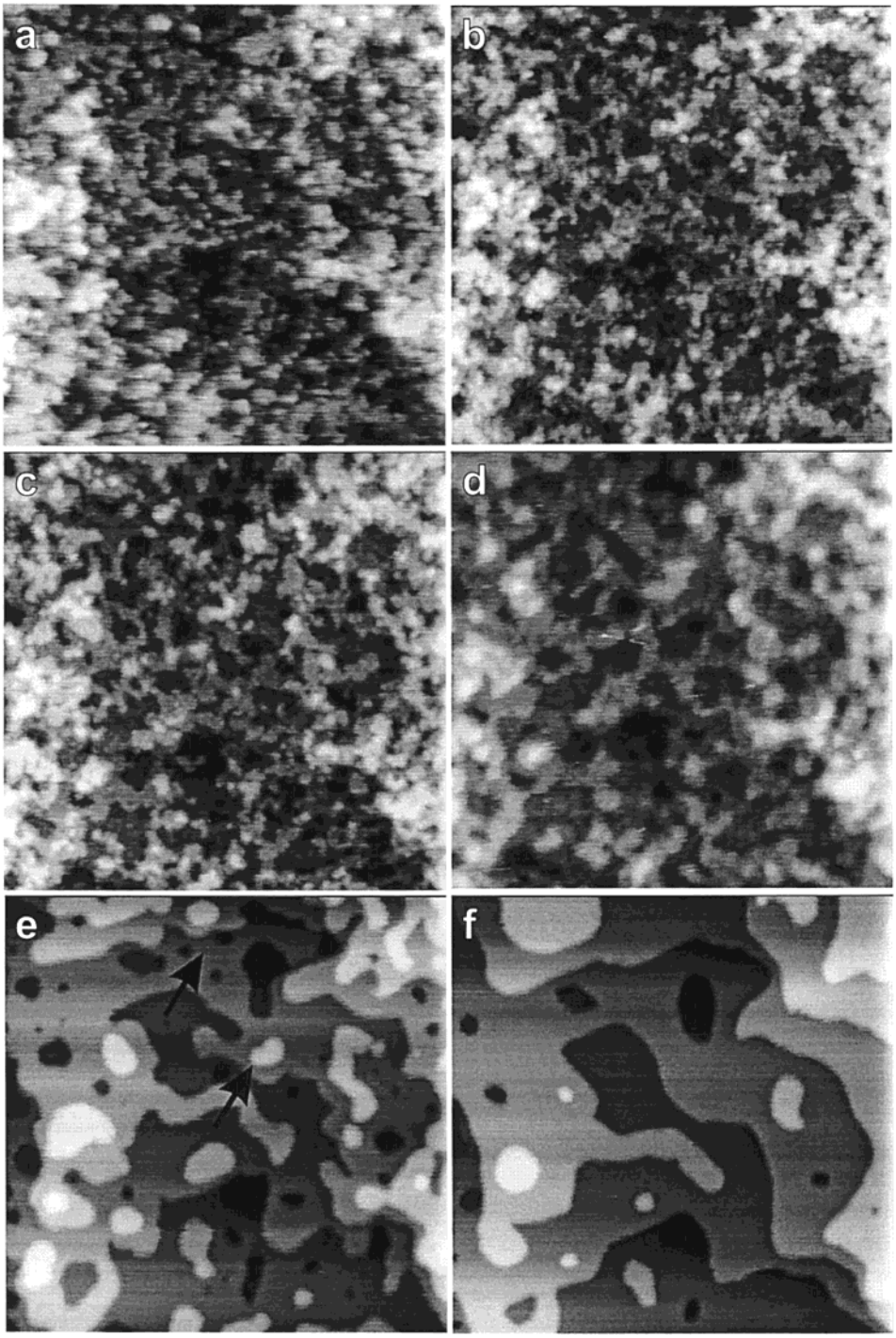

Figure 7. Potential-dependent surface annealing in 0.01 M H_2SO_4 + 10^{-5} M BTAH (1500 × 1500 Å^2, I_t = 1 nA) showing (a) the rough surface at −0.06 V (0 min, identical to Figure 5d) and increasing surface annealing after stepwise potential decrease to (b) −0.19 V (11 min), (c) −0.25 V (22 min), (d) −0.48 V (50 min), (e) −0.50 V (61 min), and (f) −0.60V (78 min).

seems to prevent the sulfate adlayer from ordering. Our model for the disordered phase would also easily explain why this phase emerges simultaneously with the onset of Cu dissolution and why it is found preferentially on the lower terrace side of the retracting steps, i.e., of dissolving terraces. In the process of Cu dissolution the reconstructed Cu top layer is removed and the next-lower (unreconstructed) Cu layer, i.e., a (1 × 1) lattice, is exposed on the lower terrace side of the step. The formation of the ordered sulfate adlayer structure, including the reconstruction of the underlying Cu surface layer, is very slow and might be even further hindered during Cu dissolution because of the presence of mobile Cu adatoms on the surface. Hence, at sufficiently high potential the terraces are dissolved more quickly than the freshly exposed surface can reconstruct. As a result, the unreconstructed areas will spread over the entire surface. In fact, a detailed inspection of the complete series shown partly in Figure 3 reveals that the shape of the disordered areas often resembles the original shape of the terraces prior to Cu dissolution (see, for example, the domain in the upper left corner of Figure 3a−d), suggesting that the rate of adlayer ordering is negligibly small in this potential regime. Alternatively, the disordered areas might also represent a highly defective, but locally reconstructed, sulfate adlayer phase. Both of these explanations are essentially similar in that the formation

of a well-ordered reconstructed surface on freshly exposed Cu surface areas is kinetically hindered, resulting in either an unreconstructed or a locally reconstructed surface with no long-range order in these areas. In very recent experiments Broekmann et al.[35] found a similar disordered phase after a fast potential step to the upper end of the double layer regime, i.e., for a sulfate adlayer formed at very similar potentials. It is noteworthy that a small fraction of the disordered phase is located also in surface areas that were not freshly exposed by removal of the topmost Cu layer. Such areas can be found, for example, at domain boundaries of the ordered sulfate adlayer. In addition to the kinetic effects discussed above, this may suggest that the ordered sulfate adlayer also has a lower stability under these conditions.

The second point that needs to be clarified is the nonuniform behavior of the dissolution process. This phenomenon can be attributed to a stabilization of the steps by the ordered sulfate adlayer. As observed by us and others,[23,24] the reconstructive ordering of the sulfate adlayer induces a faceting of the Cu steps, with the steps preferentially oriented parallel to the Moiré pattern but with no pronounced preference for one of the three possible orientations of the close-packed rows ("$\sqrt{3}$" direction) formed by the sulfate adlayer. In a simple picture these steps are particular favorable because they correspond to close-packed directions of both the reconstructed and unreconstructed Cu lattice, allowing a smooth transition from the reconstructed surface layer on the lower side of the step to the unreconstructed lattice in the same Cu layer on the higher terrace side of the step. Similar faceting effects, but even more pronounced, were reported for ordered adlayers of other strongly chemisorbed anions, such as Cl^- on Cu(100)[8−12] and Cu(111),[7] I^- on Ag(100),[36] and S on Ni(100).[37] For these systems the ordered adlayer was shown to stabilize the steps against metal dissolution with the removal of atoms proceeding solely at defects (kinks) in these steps.[10] For the Cu(111)/sulfate system the situation is qualitatively the same, but there are important differences in the detailed structure. Because of the complex structure of the sulfate adlayer and the underlying reconstructed Cu surface layer, the atomic structure along the steps is much more heterogeneous, leading to a much higher density of active sites. Consequently, the dissolution process should be less inhibited. Our observations show that the most stable steps are again parallel to the Moiré pattern, i.e., oriented along one of the close-packed directions of the underlying reconstructed Cu layer. In this case, however, there is a pronounced effect also of the sulfate adlayer orientation. Steps running perpendicular to the close-packed direction of the sulfate adlayer ("$\sqrt{3}$" direction) on the lower terrace side are most stable. This phenomenon is of general importance, since step stabilization by the lower terrace adlayer rather than by the adlayer on the upper, dissolving terrace has not yet been discussed so far. Nevertheless, this effect may be relevant also for other systems, e.g., for the anisotropic island shapes created during Cu(100) dissolution in HCl solution.[10] In that case the stability of the ⟨100⟩ steps is governed by the phase relation between the $c(2 \times 2)$ adlayer on the upper and lower terrace levels.

At later stages of the dissolution process, the lower terrace areas in the vicinity of the dissolving steps are in the disordered phase. Hence, the steps can no longer be stabilized by the ordered adlayer on the lower terrace side and their dissolution can proceed more rapidly. The presence of the disordered phase has consequences also on the local Cu step flow growth processes observed during dissolution, which can be attributed either to redeposition or to Cu transport on the surface or along the steps. Growth on the reconstructed substrate requires the transformation of the entire Cu surface layer into a (1×1) lattice. In contrast, on the unreconstructed or only locally reconstructed surface associated with the disordered phase, all or a considerable fraction of Cu surface atoms already occupy pseudomorphic lattice sites, which should allow a more facile growth than on reconstructed surface areas. This is supported by the observation of enhanced step fluctuations in disordered areas in the STM measurements.

4.2. Cu(111) in BTAH-Containing Sulfuric Acid Solution. As shown by the STM data, the ordered sulfate adlayer does not prevent the adsorption of BTAH on the Cu(111) surface. Our observations indicate the formation of a poorly ordered adlayer phase containing individual BTAH chains with a distance of ∼4 Å between neighboring BTAH molecules along the chain. The close intermolecular spacing suggests a parallel stacking of the molecular planes along the chains and hence a perpendicular (or slightly tilted) orientation of the molecules on the Cu surface. A very similar adsorption geometry was found in ultrathin films of the Cu(I)BTA multilayer phase on Cu(100).[27,29] On the other side, distinct differences are found in the chemisorption behavior of BTAH on Cu(100) and Cu(111) in H_2SO_4 solution. First, even at saturation coverages the BTAH adlayer on Cu(111) is highly defective with the BTAH molecules being arranged in small islands, whereas the chemisorbed BTAH adlayer on Cu(100) appears rather homogeneous under these conditions. Second, while on Cu(100) two-dimensional, ordered BTAH adlayers with commensurate structures are found; only the disordered, chainlike arrangement is observed on Cu(111). Third, on Cu(100) BTAH is adsorbed in the entire double layer potential range down to potentials at the onset of hydrogen evolution, whereas on Cu(111) the STM observations give no evidence of BTAH adlayer at potentials below −0.40 V.

We propose that these differences are caused by the structural differences between the sulfate adlayer structure on the two surfaces, i.e., the presence of an ordered sulfate adlayer on (reconstructed) Cu(111) compared to the mobile, disordered adlayer on Cu(100).[10] The chemisorption of BTAH on the surface covered by the ordered sulfate adlayer involves the (at least local) displacement of sulfate from the Cu surface. As evidenced by the STM experiments, in particular by those at low BTAH concentrations, this process is kinetically hindered on extended domains of the ordered sulfate adlayer. It can occur easily, however, at defects such as domain boundaries or steps. Either along with the replacement process or shortly after that the sulfate-induced and -stabilized reconstruction is removed, resulting in a highly defective Cu surface layer. This explains both the high defect density as well as the absence of two-dimensionally ordered structures in the BTAH adlayer. Occasionally, however, BTAH-covered areas were observed that still exhibited the Moiré pattern characteristic for the Cu reconstruction and that also appeared rather smooth. Apparently in certain cases a (metastable) reconstructed Cu layer can be maintained beneath the BTAH adlayer. Finally, in the potential regime where the Cu(111) surface does not exhibit the ordered sulfate adlayer phase, STM observations show no evidence of adsorbed BTAH. On Cu(100), in contrast, ordered BTAH phases are observed at similar potentials and BTAH concentrations. While a detailed microscopic explanation for these observations is still lacking, they might be related to the difference in the potential of zero charge, which should be higher on Cu(111) than on the more open Cu(100) surface.

The BTAH adlayer has drastic consequences on the mech-

anism of Cu dissolution. Instead, exclusively via a step flow mechanism it now predominantly proceeds via formation of monatomic pits, which probably are formed at defects in the BTAH adlayer. The modification in the dissolution behavior is very similar to that found for the Cu(100) phase in H_2SO_4 containing BTA[27] with the only exception that the first etch pits appear at about 50 mV more negative potentials on Cu(111) than on Cu(100). This difference may be attributed to the higher defect density in the BTAH film on Cu(111). The preference for pit formation rather than step flow etching can be understood from the stabilization ("passivation") of steps against dissolution by adsorbed BTAH species, which is effective already at submonolayer amounts of BTAH. Pit formation occurs on both BTAH-covered areas as well as on areas where the ordered sulfate overlayer is still present (see Figure 6). On the partly BTAH-covered surface pit formation commences at the same potential as on the fully BTAH-covered surface. Hence, even on the apparently fully BTAH-covered surface some small areas between the BTAH islands may still be in the ordered sulfate adlayer phase, and these areas may serve as nucleation centers for the dissolution process.

In contrast to the STM experiments, the polarization measurements showed no difference in the inhibition efficiency of BTAH on Cu(111) and Cu(100). This is probably related to the different experimental conditions in these experiments, in particular to the very different ratio of electrode surface area to the volume of electrolyte solution. In the STM cell, where this ratio is large, the BTAH coverage is limited by the amount of BTAH in solution ($\theta_{max} \approx 1$ ML for the concentration of 10^{-5} M used typically). In contrast, in the cell used for the electrochemical measurements this ratio is about 3 orders of magnitude larger, which allows the formation of Cu(I)BTA multilayer films even at a BTAH concentration of 10^{-6} M, at least in the potential range close to Cu dissolution. The different experimental conditions in STM and polarization measurements, leading to (sub-) monolayer BTAH films in the first and multilayer films in the second at similar concentrations and potentials, could account for the different results by these two techniques. The differences between Cu(100) and Cu(111) agree then with expectations, since the structure and hence the inhibition efficiency of the BTAH adlayer on Cu(111) and Cu(100) differ most strongly at submonolayer coverages but should be very similar for multilayer films. It is noteworthy that also the protection ability of submonolayer coverages is of some practical importance, since high surface-to-volume ratios are not uncommon for many technical applications of corrosion inhibitors.

5. Conclusions

The STM and electrochemical results presented in this work lead to the following conclusions on the surface structure and anodic dissolution of Cu(111) in pure and BTAH-containing sulfuric acid solution.

1. In pure H_2SO_4 solution a complex sulfate adlayer structure is formed, which apparently induces a reconstruction of the topmost Cu layer, in agreement with previous results.[23−26] This phase induces an orientation of the Cu steps parallel to the close-packed directions of the underlying reconstructed Cu surface layer.

2. Anodic Cu dissolution in pure H_2SO_4 solution commences via a step flowing mechanism, with the local dissolution rate at a step depending on the relative orientation of the sulfate adlayer on the adjacent lower terrace. Particularly stable are steps that run perpendicular to the close-packed "$\sqrt{3}$" direction of the sulfate adlayer on the lower terrace side.

3. Along with the onset of Cu dissolution an apparently disordered phase emerges, which slowly replaces the ordered sulfate adlayer and which is attributed to a disordered sulfate adlayer on top of an unreconstructed or an only locally ordered, reconstructed Cu lattice.

4. BTAH adsorbate species are observed only in the potential regime of the ordered sulfate adlayer, where they replace the sulfate adlayer. In the BTAH adlayer a poorly ordered arrangement of short chainlike molecular structures is resolved in some areas, similar to the Cu(I)BTA phase on Cu(100). The BTAH adlayer is highly defective, which is attributed to a transformation of the underlying reconstructed Cu surface layer into an unreconstructed surface. In some cases, however, the BTAH adlayer phase exists in areas where the underlying Cu reconstruction apparently is maintained.

5. BTAH inhibits the fast step flow dissolution of the Cu(111) surface and shifts the onset of dissolution by 50 to 300 mV, depending on the BTAH concentration and coverage. At more anodic surface potentials dissolution commences via nucleation and growth of monatomic etch pits, which probably form at defects in the BTAH adlayer, resulting in a roughening of the Cu surface.

6. When the potential is changed back from the dissolution into the double layer regime, the rough surface is smoothed at a rate that increases strongly with decreasing potential, whereas in pure H_2SO_4 solution Cu redeposition occurs via nucleation and growth of Cu islands.

7. Although the mechanisms of Cu dissolution in BTAH-containing H_2SO_4 solution are similar on Cu(100) and Cu(111), the latter apparently is less stable at submonolayer BTAH coverages. This might be related to the higher defect density in the BTAH adlayer, which in turn is caused by the structural transition in the Cu substrate during replacement of the ordered sulfate adlayer by BTAH.

Acknowledgment. We gratefully acknowledge the Deutscher Akademischer Austauschdienst (DAAD) for financial support for W.P., the Deutsche Forschungsgemeinschaft (DFG) for financial support and a fellowship for O.M.M., and the Max-Buchner Forschungsstiftung for a fellowship for M.R.V.

References and Notes

(1) Smyrl, W. H. In *Electrochemical materials science*,; Bockris, J. O., Conway, B. E., Yeager, E., White, R. E., Eds.; Plenum Press: New York 1981; Vol. 4, p 97.
(2) Mayanna, S. M.; Setty, T. H. V. *Corros. Sci.* **1975**, *15*, 627.
(3) Stickney, J. L.; Villegas, I.; Ehlers, C. B. *J. Am. Chem. Soc.* **1989**, *111*, 6473.
(4) Villegas, I.; Ehlers, C. B.; Stickney, J. L. *J. Electrochem. Soc.* **1990**, *137*, 3143.
(5) Cruickshank, B. J.; Gewirth, A. A.; Rynders, R. M.; Alkire, R. C. *J. Electrochem. Soc.* **1992**, *139*, 2829.
(6) LaGraff, J. R.; Gewirth, A. A. In *Nanoscale probes of the solid/liquid interface*; Gewirth, A. A., Siegenthaler, H., Eds.; Kluwer Academic Publishers: Dordrecht, Boston, London, 1995; Vol. E288, p 83.
(7) Suggs, D. W. Bard, A. J. *J. Am. Chem. Soc.* **1994**, *116*, 10725.
(8) Suggs, D. W.; Bard, A. J. *J. Phys. Chem.* **1995**, *99*, 8349.
(9) Vogt, M. R.; Möller, F.; Schilz, C. M.; Magnussen, O. M.; Behm, R. J.; *Surf. Sci.* **1996**, *367*, L33.
(10) Vogt, M. R.; Lachenwitzer, A.; Magnussen, O. M.; Behm, R. J. *Surf. Sci.* **1998**, *399*, 49.
(11) Moffat, T. P. *Mater. Res. Soc. Symp. Proc.* **1996**, *404*, 3.
(12) Moffat, T. P. *Mater. Res. Soc. Symp. Proc.* **1997**, *451*, 75.
(13) Cotton, J. B.; Scholes, I. R. *Br. Corros. J.* **1967**, *2*, 1.
(14) Roberts, R. F. *J. Electron Spectrosc.* **1974**, *4*, 273.
(15) Youda, R.; Nishihara, H.; Aramaki, K. *Corros. Sci.* **1988**, *28*, 87.
(16) Youda, R.; Nishihara, H.; Aramaki, K. *Electrochim. Acta* **1990**, *35*, 1011.
(17) Wu, Y. C.; Zhang, P.; Pickering, H. W.; Allara, D. L. *J. Electrochem. Soc.* **1993**, *140*, 2791.
(18) Fang, B. S.; Olson, C. G.; Lynch, D. W. *Surf. Sci.* **1986**, *176*, 476.

(19) Nilsson, J.-O.; Törnkvist, C.; Liedberg, B. *Appl. Surf. Sci.* **1989**, *37*, 306.
(20) Tromans, D.; Sun, R.-H. *J. Electrochem. Soc.* **1991**, *138*, 3235.
(21) Cho, K.; Kishimoto, J.; Hashizume, T.; Pickering, H. W.; Sakurai, T.; *Appl. Surf. Sci.* **1995**, *87/88*, 380.
(22) Cruickshank, B. J.; Sneddon, D.; Gewirth, A. A. *Surf. Sci.* **1993**, *281*, L308.
(23) Wilms, M.; Broekmann, P.; Kruft, M.; Park, Z.; Stuhlmann, C.; Wandelt, K. *Surf. Sci.* **1998**, *83*, 404−404.
(24) Wilms, M.; Broekmann, P.; Stuhlmann, C.; Wandelt, K. *Surf. Sci.* **1998**, *416*, 121.
(25) Li, W.-H.; Nichols, R. J. *J. Electroanal. Chem.* **1998**, *456*, 153.
(26) Randler, R. J.; Kolb, D. M. Unpublished.
(27) Vogt, M. R.; Polewska, W.; Magnussen, O. M.; Behm, R. J. *J. Electrochem. Soc.* **1997**, *144*, L113.
(28) Vogt, M. R.; Nichols, R. J.; Magnussen, O. M.; Behm, R. J. *J. Phys. Chem. B* **1998**, *102*, 5859.
(29) Vogt, M. R.; Magnussen, O. M.; Behm, R. J. *Electrochem. Soc. Proc.* 98-17, in press.
(30) Wiechers, J.; Twomey, T.; Kolb, D. M.; Behm, R. J. *J. Electroanal. Chem.* **1988**, *248*, 451.
(31) Polewska, W.; Vogt, M. R.; Magnussen, O. M.; Behm, R. J. Unpublished results.
(32) Magnussen, O. M.; Hageböck, J.; Hotlos, J.; Behm, R. J. *Faraday Discuss.* **1992**, *94*, 329.
(33) Wan, L.-J.; Yau, S.-L.; Itaya, K. *J. Phys. Chem.* **1995**, *99*, 9507.
(34) Funtikov, A. M.; Linke, U.; Stimming, U.; Vogel, R. *Surf. Sci.* **1995**, *324*, L343.
(35) Broekmann, P.; Wilms, M.; Wandelt, K. *Surf. Rev. Lett.*, in press.
(36) Teshima, T.; Ogaki, K.; Itaya, K. *J. Phys. Chem. B* **1997**, *101*, 2046.
(37) Ando, S.; Suzuki, T.; Itaya, K. *J. Electroanal. Chem.* **1996**, *412*, 139.